Medical Oncology (2023) 40:156
https://doi.org/10.1007/s12032-023-02027-4

ORIGINAL PAPER

LXR inhibitor SR9243-loaded immunoliposomes modulate lipid metabolism and stemness in colorectal cancer cells

Hassan Dianat-Moghadam[1,2,4] · Soheil Abbasspour-Ravasjani[3] · Hamed Hamishehkar[3] · Reza Rahbarghazi[4] · Mahammad Nouri[1,4]

Received: 28 February 2023 / Accepted: 13 April 2023 / Published online: 24 April 2023

Abstract

Reprogrammed metabolism and active stemness contribute to cancer stem cells' (CSCs) survival and tumorigenesis. LXR signaling regulates the metabolism of different cancers. A selective LXR inhibitor, SR9243 (SR), can target and eradicate non-CSC tumor cells. CD133 is a stem marker in solid tumors-associated CSCs within the active lipogenesis, and anti-CD133 mAb targeting liposomal drug delivery systems expected to increase drug internalization and improve the therapeutic efficacy of poor-in water solubility drugs, e, g., SR. In this study, anti-CD133 mAbs-targeted Immunoliposomes (ILipo) were developed for specific delivery of SR into MACS-enriched CD133 + CSCs and induce their functional effects. Results have shown that ILipo having an average size of 64.79 nm can encapsulate SR in maximum proportion, and cell association studies have shown cationic ILipo and targeting CD133 provide the CSCs binding. Also, FCM analysis of RhoB has demonstrated that the ILipo uptake was higher in CD133 + CSCs than in the non-targeted liposomes. ILipo-SR was significantly more toxic in CD133 + CSCs compared to the free SR and non-targeted ones. More efficient than Lipo-SR, ILipo-SR improved the reduction of clonogenicity, stemness, and lipogenesis in CD133 + CSCs in vitro, boosted ROS generation, and induced apoptosis. Our study revealed the dual targeting of CD133 and LXR appears to be a promising strategy for targeting CD133 + CSCs-presenting dynamic metabolism and self-renewal potentials.

✉ Hassan Dianat-Moghadam
dianat.h@med.mui.ac.ir

✉ Mahammad Nouri
Nourimd@yahoo.com

1 Department of Medical Biotechnology, Faculty of Advanced Medical Sciences, Tabriz University of Medical Sciences, Tabriz, Iran

2 Department of Genetics and Molecular Biology, School of Medicine, Isfahan University of Medical Sciences, Isfahan, Iran

3 Drug Applied Research Center, Tabriz University of Medical Sciences, Tabriz, Iran

4 Stem Cell Research Center, Tabriz University of Medical Sciences, Tabriz, Iran

Graphical abstract

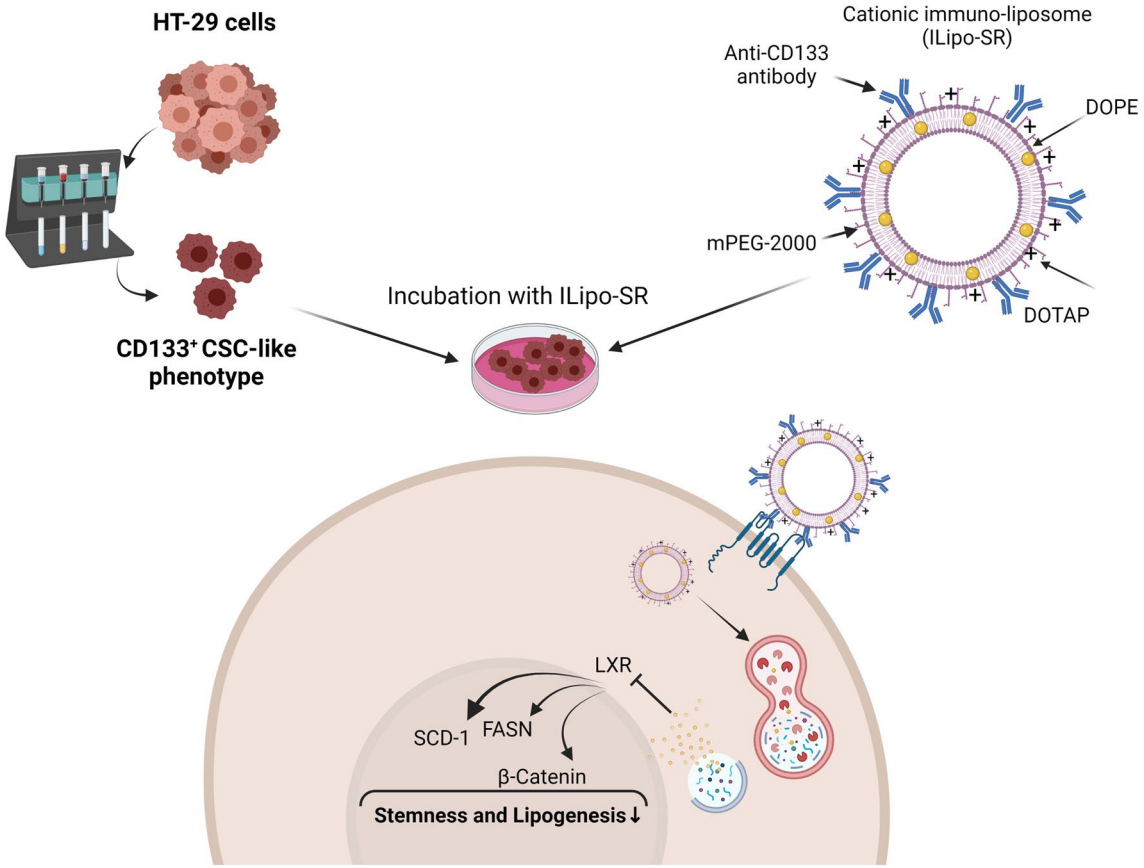

Keywords Cancer metabolism · Clonogenicity · LXR · ROS · Stemness

Abbreviations

CSC	Cancer stem cell
CLs	Cationic liposomes
DOPE	Dioleoyl phosphatidylethanolamine
DOTAP	1,2-Dioleoyl-3-trimethylammonium-propane
FASN	Fatty acid synthase
ILipo	Immunoliposomes
LXR	Liver X nuclear receptor
MACS	Magnetic activated cell sorting
SCD1	Stearoyl-CoA desaturase-1

Background

Cancer stem cells (CSCs) are recognized with the ability to self-renew, promote tumor metastasis and induce tumor recurrences after chemotherapy [1]. Identifying and specific targeting of CSCs requires understanding their broader biological traits such as metabolic pathways [2]. CSCs survival demands a highly active metabolic program such as aerobic glycolysis and lipogenesis [1, 3]. Lipids play a crucial role in CSC propagation and support membrane integrity and the function of membrane-localized proteins [2]. Higher levels of lipid unsaturation in $ALDH^+/CD133^+$ CSCs related to enhanced de novo synthesis of lipids mediated by overexpressed fatty acid desaturase Δ9 (or SCD1, stearoyl-CoA desaturase-1) [3]. Subsequently, elevated SCD1 contributes to the maintenance of cancer cell stemness and induces sphere growth and tumorigenesis [3].

As reported in colorectal cancer (CRC), the high-fat diet and dysregulated WNT signaling pathway drive malignant transformations in $Lgr5^+$CSCs [4]. On other hand, Liver X nuclear receptor (LXR) is a nuclear transcription factor activated by oxysterol metabolites to regulate lipid homeostasis [5]. Activated LXR modulates cholesterol uptake and de novo lipogenesis which sustains cell proliferation and resistance to cellular stress [6]. Therefore, manipulating the lipids biosynthesis pathway through modulating the LXR signaling pathway could act as a potential strategy to target CR-CSCs.

Nonetheless, the delivery of LXR modulators and elimination of CR-CSCs demand targeted therapy due to the lack of specificity of the administrated drugs and poor-in water solubility of such drugs. CD133 as membrane-located glycoprotein participates in regulating membrane-associated signaling pathways involved in stemness, growth, and even cholesterol hemostasis in solid tumors-associated CSCs [7–9]. Therefore, targeting CD133 given the specificity and perfect candidates in the development of nanocarrier-based targeted therapies. Liposomes are biocompatible nanocarriers that hold considerable potential in cancer therapy through simple loading and chemical conjugates [10]. In this respect, liposome-encapsulated paclitaxel (Nano-Taxol) was utilized to target metabolic reprogramming in CSCs. Results have shown Nano-Taxol effectively suppressed stemness-induced the glycolysis switching to oxidative phosphorylation status with potent elimination of ovarian CSCs [11]. Off-target delivery and low stability clues impair the delivery efficacy of simple liposomal formulations which is addressed through passive targeting and active targeting to facilitate intracellular transport and delivery of drugs [10, 12]. The decoration of DOX-loaded PEGylated Liposomes with anti-CD44 antibody [13], or aptamer [14], can simultaneously bind to overexpressed CD44 markers on cancer cells and then internalized DOX into the cytoplasm through receptor-mediated endocytosis. Additionally, targeting CD44 and CD133 can selectively and specifically target and deliver therapeutic agents into solid cancer-associated CSCs [15, 16].

SR9243 (or N-[2-(3-Bromophenyl)ethyl]-2,4,6-trimethyl-N-[[3′-(methylsulfonyl)[1,1′-biphenyl]-4-yl]methyl]benzenesulfonamide) acts as an enzyme-specific inhibitor drug that selectively targets and downregulates LXR activity through inducing LXR-corepressor interaction and thus, modulates LXR-mediated gene expression involved in downstream Warburg effect or glycolysis pathway and a variety of proteins that regulate lipid metabolism in tumor cells [17]. This study aimed to prepare CD133-targeted PEGylated ILipo containing LXR reverse agonist SR9243 (ILipo-SR) based on that knowledge and then study its effects on the growth, stemness, metabolism, and colony formation of HT-29-isolated $CD133^{+}$CSCs in vitro. We hope this work can shed light on the development of new ideas and approaches to treat CRC based on CSCs targeting.

Materials and methods

Materials

DOTAP (1,2-dioleoyl-3-trimethylammonium-propane) and DOPE (1,2-dioleoyl-sn-glycero-3-phosphoethanolamine) was purchased from Avanti Polar Lipids (Alabaster, AL, USA). SR9243 provided by TOCRIS (China). Anti-CD133 mAb purchased from abcam (ab19898, Cambridge, UK). FITC-conjugated anti-human CD133 antibody (Clone: AC133; Cat No. 130–113-673), Microbeads against CD133 and MACS-LS columns purchased from Miltenyi Biotec (Germany). RPMI 1640, Fetal Bovine Serum (FBS), Penicillin, Streptomycin, Trypsin–EDTA, and 4′,6-diamidino-2-phenylindole (DAPI) provided by Gibco (USA). Amicon® provided by Millipore (Germany). (3-(4, 5-Dimethylthiazol-2-yl)-2, 5-Diphenyltetrazolium Bromide (MTT), Rhodamine B (RhoB), Phosphate buffered saline (PBS), Dimethyl sulfoxide (DMSO, 99.9%), and bovine serum albumin (BSA) purchased from Sigma-Aldric (USA). Primary and secondary HRP-conjugated antibody provided by Santa Cruz Biotechnology (Santa Cruz, USA). Annexin V-FITC/PI (Propidium Iodide) and binding buffer provided by Beyotime Biotechnology (Shanghai, China). Chamber slides, 6/12/96-well plates were purchased from SPL(Korea). HT-29 cell line was purchased from the National Cell Bank of Iran (NCBI; Pasteur Institute, Tehran).

Preparation and characterization of liposomal formulations

Multilamellar vesicles (MLVs) were generated using a technique based on the established film method and modified for low-solubility drugs. Briefly, the lipid entities DSPE-mPEG-2000 (5% of total solvent), DOPE, and DOTAP cationic lipids (DOPE: DOTAP,1:1 M ratio) were dissolved in chloroform and the required amount of SR9243 (SR) (25 µL; 5 µM) as selected drug added to lipids, and then the solvent evaporated on a rotary evaporator to yield a dry film as per the standard lipid film hydration method. The film was hydrated with 300 mM of citrate buffer, pH 5.5, to give a final drug concentration of 0.2 M as stock solutions. To prepare small unilamellar vesicles (SUV), the MLVs were subjected to hear force-induced homogenizer (20,000 rpm for 20 min at 50–60 °C of bathwater), and probe sonication for 5–10 sonication cycles (60 s/cycles) with 60 s stop time between each sonication cycle using a Bioruptor® Plus sonicator at 4 °C to form SR-loaded PEGylated liposomes (or Lipo-SR).

The role of DOTAP in the prepared cationic liposomes (CLs) was providing cationic lipid nanoparticles, which conducted the electrostatic interaction between the negatively charged anti-CD133 mAbs (1 mg/mL, pH 7.4) and catatonic lipid DOTAP to produce modified Immunoliposomes (anti-CD133-ILipo) in a post-insertion method. Briefly, the anti-CD133 mAbs were added into 5 mL of pre-formulated Lipo-SR at a molar ratio of 100:1 (DOTAP/mAbs) to form liposomes while being shaken gently for one h at 4 °C. Anti-CD133 ILipo-SR was obtained following purification by dialysis.

The sizes, zeta potential, and polydispersity index (PDI) of Lipo-SR and ILipo-SR were determined by a dynamic light scattering (DLS) system using the photon correlation spectroscopy (PCS) technique measured on a Malvern Zetasizer Nano-ZS (Malvern Instruments Ltd., UK). Using the cuvettes supplied by Malvern, 100 µL of the sample was diluted by freshly filtered hydration phase (*i.e.*, 1:100 v/v PBS or dH_2O) up to 1 mL, and the zeta potential, vesicle size, and PDI were measured at 25 °C. Furthermore, to investigate the morphology and core–shell structure of prepared nanocarriers, transmission electron microscopy (TEM) was used (Zeiss NEO-906, 100 kV Germany).

Entrapped SR assay

The amount of SR entrapped in the liposomal nanoparticles was determined by filtering the formulation through Amicon centrifugal tubes (30 K) for 3000 rpm 10 min to remove the free drug not bound to liposomes. After dialysis, free drugs not bound to liposomes were analyzed using UV-HPLC (Knauer, Germany) to calculate drug unloading at the 258 nm wavelength for SR. A Luna 5 µ C8, 40 mm × 4.6 mm 100 A, Phenomenex column was used to for HPLC separation using acetonitrile (ACN) and water (80:20 v/v) as the mobile phase was run at 1 mL/min and the absorbance was read at 258 nm. Standard calibration curves of the drug were used to calculate free drug not bound to liposomes.

Cell culture, MACS, and characterization of isolated cells

Human colorectal adenocarcinoma cell line HT-29 was cultured in RPMI 1640 medium supplemented with 10% v/v FBS, 100 IU/mL Penicillin, and 100 µg/mL Streptomycin. In the current experiment, CSCs were enriched based on stemness surface marker CD133 using MACS (Magnetic Activated Cell Sorting) according to the manufacturer's instruction [5]. In short, the adherent HT-29 cells at 70–80% confluency were harvested using 0.25% trypsin–EDTA and washed twice with PBS. The nonspecific binding sites were blocked with 1% BSA. To isolate $CD133^+$ cells, HT-29 cells (30×10^6) were incubated with 100 µL of microbeads against CD133 at 4 °C for 20 min on a rotator. After that, cells were washed with PBS containing 1% BSA and passed through the LS column. Soon after enrichment, $CD133^+$ cells were collected as primary CSCs for subsequent studies. To confirm the purity of enriched CSCs, we performed flow cytometry (FCM) assays of CD133. The LS-enriched cells were washed twice with PBS and incubated with 10 µL of the FITC-conjugated anti-human CD133 antibody at 4 °C for 30 min. Then, cells were washed twice with PBS, resuspended in PBS, and analyzed using a FACSCalibur flow cytometer (BD Bioscience, USA) and FlowJo software (version 7.6.1). The purity of cells expressing CD133 was compared with control HT-29 cells before the MACS procedure.

Cellular binding of FITC-CD133 mAbs-targeting Liposomes

Specific binding of Immunoliposomes to sorted $CD133^+$ CSCs and pre-MACS HT-29 cells was performed using fluorescence microscopy. The CSCs were seeded in 8 well chamber slides for 24 h, and then treated with FITC-CD133 mAbs-conjugated ILipo (with or without SR) and incubated for 15 min at 37 °C. After being washed three times with PBS, the treated cells were treated with 2% cold paraformaldehyde for 15 min, stained with DAPI for 10 min at 25 °C in a dark room, and finally, examined using a fluorescence microscope. Moreover, the binding of anti-CD133 Ab to the surface of liposomes was evaluated using the silver staining method as reported previously [18].

In vitro cellular uptake assay

FCM study assessed Lipo and ILipo uptake. The lipid composition and hydration step are similar to Lipo-SR preparation for fluorescent liposomes. For this purpose, the formulations were prepared without drugs, containing the fluorescent lipid core marker, RhoB, encapsulated at 0.5% v/v. To separate the free RhoB from entrapped RhoB, a purification process was applied using an Amicon® tube (Ultra-30 kDa molecular weight cut-off membrane). The fluorescent liposomes were placed into the upper chamber of Amicon® Falcon and centrifuged at 3000 rpm for 15 min. Unloaded RhoB molecules were passed through the filter and gathered in the lower chamber of the Amicon tube. The upper chamber that comprised pure fluorescent liposomes was diluted with PBS and then centrifuged three times again to ensure the total removal of non-entrapped RhoB from the nanoparticles. To prepare ILipo-RhoB, anti-CD133 mAbs were conjugated by the same procedure used for conjugation in ILipo-SR. After that, the $CD133^+$ CSCs were seeded 2×10^5 cells/well in 12-well plates and incubated at 37 °C in 5% CO2 for 24 h. After that, cells were treated with fluorescent RhoB-loaded Lipos and ILipo for 1, 2, 4, 8, 12, and 24 h.; they were washed twice with sterile PBS and collected by centrifugation, and followed by being resuspended in 500 µL PBS. Finally, the quantitative cellular uptake of the formulations was analyzed using the FACSCalibur flow cytometer (BD Bioscience, USA) and FlowJo software (version 7.6.1).

Cell viability assay

The effect of free SR, Blank Lipo, Lipo-SR, and ILipo-SR was determined on CSC viability by a colorimetric assay using MTT. Briefly, 1.5×10^4 CSCs resuspended in a culture medium enriched with 2% FBS and transferred onto each well of 96-well plates. After 24 h, cells were exposed to various concentrations of formulated SR (50–500 nM). After completing the treatment protocol for 48 h, 50 µL of MTT (2 mg/mL) solution was added to each well and incubated for the next 4 h. Thereafter, the culture medium was removed and replaced with 200 µL DMSO solution. Finally, the absorbance value was measured at 630 nm using a microplate reader (BioTeK Instruments, USA). The data was analyzed, and the IC_{50} value was obtained using GraphPad Prism software (Version 9.0.0).

Western blot analysis

To study the impact of different SR preparations on CSC metabolism and stemness, we used WB to analyze relevant genes expression in $CD133^+$ CSCs. Following the completion of cell treatment Blank Lipo/Lipo-SR/ILipo-SR, CSCs were lysed in a protein extraction buffer composed of 25 mm HEPES, 1% Triton X-100, 2 mM EDTA, 0.1 M NaCl, 25 mM NaF, 1 mM Sodium Orthovanadate and protease cocktail inhibitor (Roche) on ice for 30 min. Cell lysates were centrifuged at 12,000 g for 20 min at 4 °C. Then, the total protein concentration of supernatants was measured using Nanodrop®. The samples were electrophoresed by 12.5% SDS-PAGE and transferred to PVDF membrane. A 5% skim milk solution was used to block nonspecific binding sites. In this study, membranes were incubated with primary antibodies at 4 °C overnight. An appropriate secondary HRP-conjugated antibody was applied for 1 h at room temperature. Finally, immunoreactive bands were detected by using ECL reagent (BioRad). The density of each band was determined using ImageJ software (ver. 1.4).

Clonogenicity assay

The colony formation assay was performed to investigate the effect of the Blank Lipo, Lipo-SR, and ILipo-SR on the clonogenicity of $CD133^+$CSCs. That, 1×10^3 CSCs/well cells were seeded in a six-well plate after 24 h incubation. They are treated with mentioned formulations based on their IC_{50} obtained by MTT assay. Following 14 days of culture, the colonies were stained with crystal violet 2% for 15 min, and then photographed. They were counted manually and plotted as the number of colonies.

Intracellular ROS assay

The reactive oxygen species (ROS) level was evaluated using 2′, 7′-dichlorofluorescein diacetate (DCFH-DA) staining and FCM assay. In brief, 1×10^6 $CD133^+$CSCs were seeded in 6-well plates and treated with blank Lipo, free SR (113 nM), Lipo-SR (87 nM), ILipo-SR (43 nM), and hydrogen peroxide (H_2O_2) as a positive control. After 48 h, CSCs were incubated with 10 µg/mL of DCFH-DA for 60 min. After that, cells were trypsinized, washed, and resuspended in PBS. Finally, the FCM assay used 1000 events per sample using Fl2-H band-pass filter (FITC). The data were analyzed by FlowJo software (ver. 7.6.1), and the fluorescence intensity of the treatment groups was compared to each other.

Apoptosis assay

The percent of apoptotic CSCs was determined after LXR inhibition via FCM analysis of Annexin V-FITC/PI double staining assay. After 48 h treatment with Blank Lipo, free SR, Lipo-SR, or ILipo-SR, cells were collected and washed twice with PBS, and resuspended in binding buffer at 4 °C for 20 min followed by incubation in 10 µg/mL Annexin V-FITC that targets PS (phosphatidylserine) molecules present on the outside layer of apoptotic cell membranes and 5 µL of PI. This fluorescent DNA intercalant molecule stains nuclear DNA when cells undergo late apoptosis/necrosis. CSCs were incubated at 4 °C for 20 min and then washed in 2 mL of binding buffer. CSCs were then centrifuged and the cell pellet was resuspended in 500 µL of binding buffer. The percent of apoptotic CSCs was determined using the BD FACSCalibur and FlowJo software (ver.7.6.1).

Statistics

Statistical evaluation was performed through one-way and two-way ANOVA. All data are expressed as the mean ± standard deviation (SD) unless otherwise noted. A value of $p < 0.05$ was considered statistically significant.

Results

Liposome's characterization

According to DLS analysis, the PDI, particle size and zeta potential value of Lipo-SR were 0.25, 62.79 nm, and + 26 mV, respectively (Fig. 1a-b). DLS analysis reported the PDI, hydrodynamic diametric, and zeta potential value of ILipo-SR 0.49, 64.79 nm, and + 22.1 mV, respectively (Fig. 1d, e). The IgG Ab like anti-CD133 mAb bears negative charges in PBS buffer (pH 5) [19], therefore, it is presumable the ILipo would have more negative surface charges

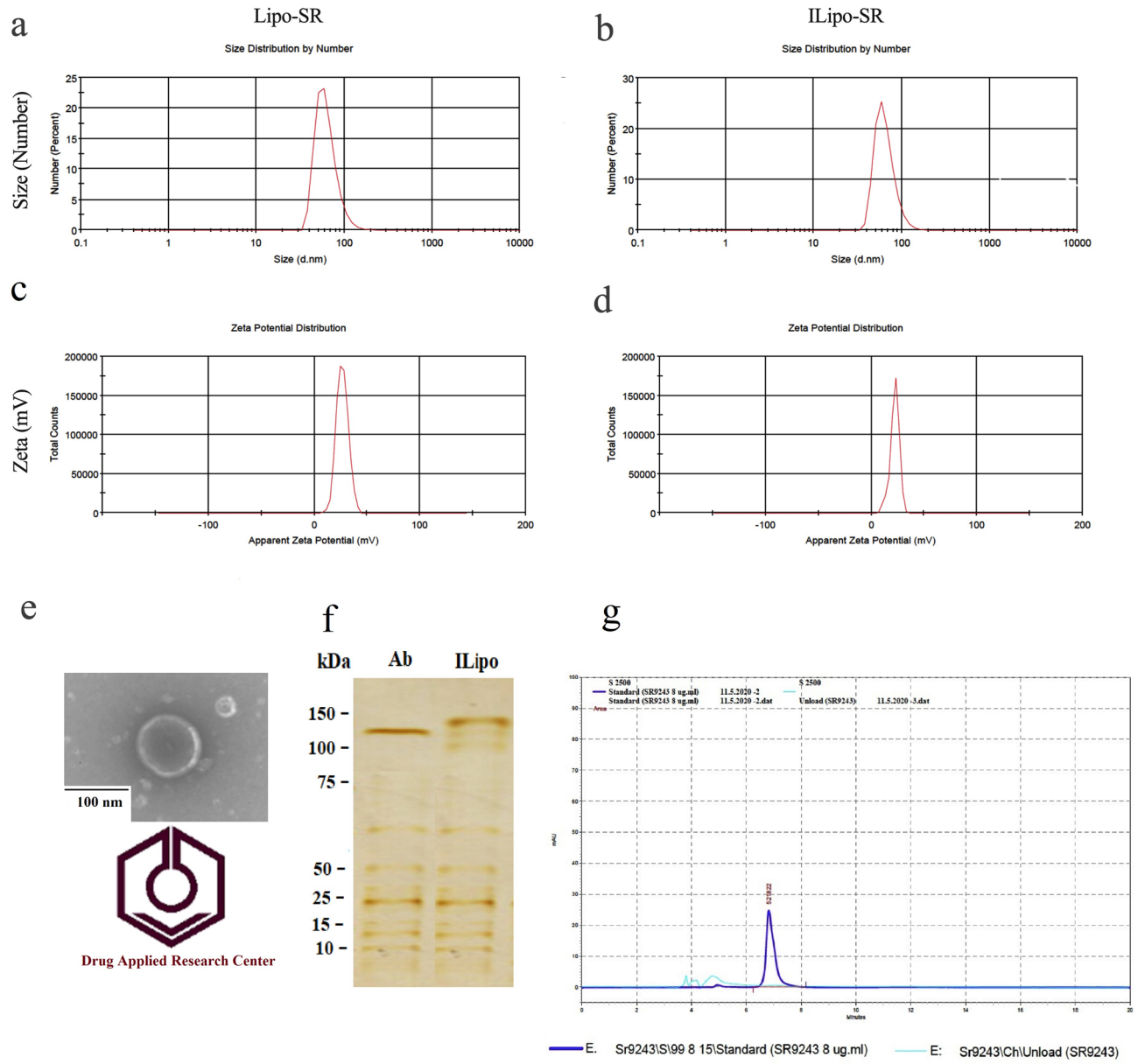

Fig. 1 DLS obtained particle size and zeta potential for Lipo-SR (**a-b**) and ILipo-SR (**d, and e**). TEM results of prepared nanostructured ILipo-SR (**c**). Silver staining result of anti-CD133 mAbs and ILipo (**f**). Loading study of the SR9243 (SR) by analysis of the absorption of free SR in unloaded liposomes at 258 nm using UV-HPLC chromatogram (**g**). The chromatogram of standard (dark blue) and unladed SR-liposomes (pale blue) after filtering the formulation through Amicon centrifugal tubes. DLS, dynamic light scattering; ILipo, Immunoliposomes; Lipo, liposomes; SR, SR943; TEM, transmission electron microscopy (Color figure online)

than normal Lipo, and a reduction of the positive charge of Lipo-SR from + 26 to + 22.1 mV in ILipo-SR indicated the effect of negatively charged anti-CD133 mAbs on cationic lipid DOPE, and thus, confirmed the occupancy and presence of conjugated anti-CD133 mAbs on the surface of Lipo-SR to produce CD133-ILipo. However, there were no significant differences in average particle sizes between Lipo-SR and ILipo-SR. Furthermore, TEM also revealed that prepared nanoparticles had liposomal morphology and confirmed formulations size reports ensuring that CD133-ILipo had the acceptable size for drug delivery (Fig. 1c). Silver staining demonstrated the binding of antibody to liposomes (Fig. 1f), and then, UV-HPLC analysis showed any absorbance of free drug not bound to liposomes SR at 258 nm, which indicated full encapsulation of SR into liposomal formulation as an expected duo the very small of used SR in compares to used lipid components that used in liposomal structure (Fig. 1g).

FCM confirmed the purity of MACS-isolated CSCs

CD133 is a potentiated stem cell marker within the most typical future of colon carcinoma [20], and thus, we performed MACS analysis to enrich CSCs from the human HT-29 cell line (Fig. 2a) through applying specific anti-CD133$^+$ antibodies. Then, FCM was performed to confirm the purity of CSCs. Direct quantification of the CD133$^+$ cell population revealed that about 98.7 ± 4.2% of MACS-isolated cells expressed CD133$^+$ surface marker (Fig. 2b), showing that a large proportion of enriched cells exhibited CSC-like phenotype (Fig. 2c). These data showed the successful isolation and identification of CSC subpopulation from total HT-29 cells.

Anti-CD133 mAb mediated CSCs recognition and uptake of RhoB by targeted liposomes

The conjugation of anti-CD133 mAb to the surface of PEGylated liposome and produced ILipo was detected by FITC-conjugated anti-human CD133 antibody and fluorescence microscopy. The negative control (*i.e.*, CD133 LE HT-29 cells) showed no detectable binding of FITC-CD133-ILipo fluorescence intensity afterv15 min (Fig. 3a), however, as shown in Fig. 3b coupled anti-CD133 mAbs cause the ILipo to bind selectively to CD133 overexpressed CSC antigens after 15 min, which leads to increased uptake and delivery of FITC-CD133-ILipo to the target cells. Meanwhile, CD133$^+$CSCs displayed a high affinity for the CD133 antibody coupled to the nanocarrier, with a significant increase in fluorescent intensity, compared with pre-MACS HT-29 cells.

Liposomal targeting with mAbs able to increase the uptake by cells overexpressing the related receptor. In the present work, the cellular uptake of Lipo and ILipo was evaluated at 1, 2, 4, 8, 12, and 24 h in pre- CD133$^+$CSCs (or cells with high expression (HE) of CD133 marker). As expected, the results showed significantly higher uptake of the ILipo-RhoB in the CD133$^+$CSCs compared to the non-targeted Lipo-RhoB ($p < 0.05$–0.0001), and was noticeable even after 2 h, increasing over time (Fig. 3c). Moreover, nanocarriers uptake was time-dependent, the cell uptake increased over time of incubation in MACS-enriched CD133$^+$CSC-like cells CSCs, both for the Lipo-RhoB and for the ILipo-RhoB (Fig. 3c). These results indicated the better uptake of ILipo by the CD133$^+$ cell line and emphasize the conjugation of anti-CD133 mAbs as the ligand on the surface of ILipo can specifically lead to increased coupling of ILipo-RhoB/SR to CD133 on CSCs, and subsequently increased their cellular uptake.

Liposomal SR formulations reduced the CSCs viability

CSCs are resistant to anti-proliferative chemotherapeutic agents [10], and enriched CR-CSCs were tested for their metabolism and growth inhibition by various liposomal SR (an LXR antagonist) formulations. Increased growth inhibitory effect in CR-CSCs was achieved by encapsulating SR in Lipo and more so in CD133-targeting ILipo in a dose-dependent manner (Fig. 4). According to our data, the Lipo-SR (~ 58 nM in IC_{50} value) and CD133-targeting ILipo-SR (~ 37 nM in IC_{50} value) showed the 1.3- and 2.63-fold higher cytotoxicity than free SR (~ 79 nM in IC_{50} value) on HT-29 CSCs, respectively (Fig. 4). This is presumably due to the increased solubility and delivery of poorly water-soluble SR9243 (*i.e.*, liposomal SR formulations *vs.* free SR) into CSCs. We selected IC_{50} values for subsequent analyses.

Liposomal SR modulated the metabolic and stemness phenotypes of CSCs

The reprogrammed lipogenesis contributes to CSCs' survival, metabolism, and stemness [1, 3]. Here, we

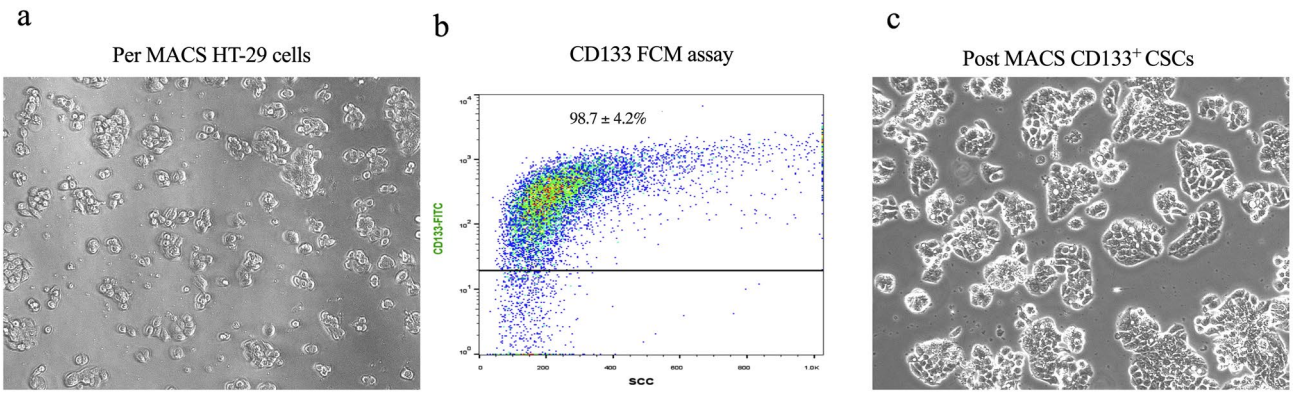

Fig. 2 CD133 + cancer stem-like cells (CSCs) were enriched from human HT-29 cell line (**a**) using magnetic activated cell sorting assay (MACS), and then FITC-conjugated anti-CD133 antibody and flow cytometry analysis was used (**b**) to assay the purity of isolated cells (**c**)

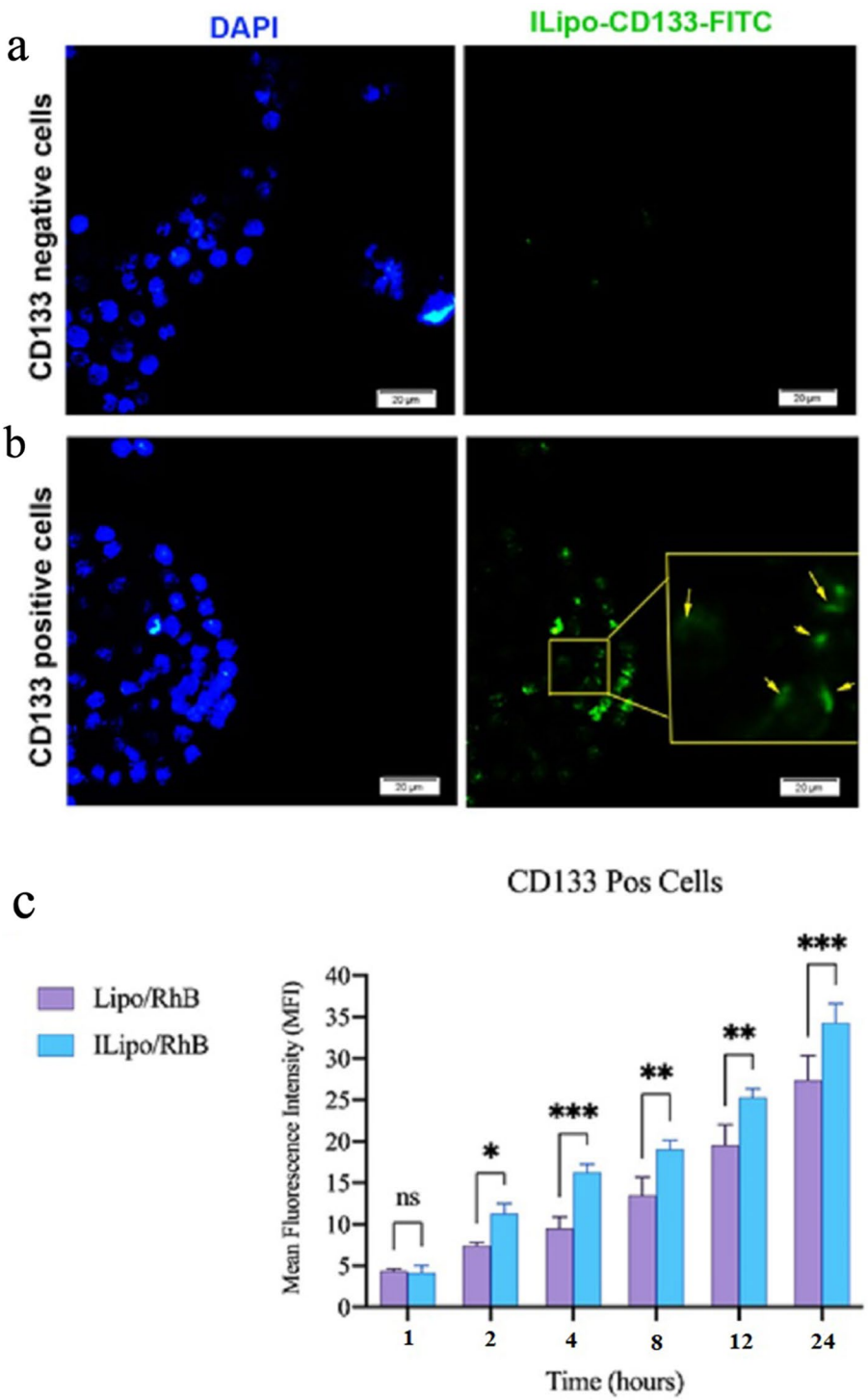

Fig. 3 Fluorescence microscopy imaging of FITC-CD133-ILipo binding to CD133 LE and HE cells after 15 min, respectively (**a**-**b**). Flow cytometry analysis of cellular uptake of RhoB labeled ILipo after 1–24 h of incubation. Histogram of CD133 + cells that were treated with different liposomal formulations of Lipo-RhoB and ILipo-RhoB. Data represent mean ± SD ($n = 3$). DAPI, 4′, 6-diamidino-2-phenylindole. HE, high expression, LE, low expression; Lipo, liposomes; RhoB, Rhodamine B

investigated whether LXR inhibition could alter the protein expression of lipogenesis SCD1 and FASN (fatty acid synthase) enzymes, the β-catenin factor of WNT pathway (presenting maintenance and propagation of CSCs), and NANOG, ALDH1 (aldehyde dehydrogenase 1), SOX2 (SRY box-containing gene-2), and OCT 3/4 (octamer-binding transcription factor 3/4) biomarkers presenting self-renew and stemness phenotype of CSCs. Here, we showed that incubation of CSCs with Lipo-SR and ILipo-SR diminished the protein level of SCD1 after 48 h, compared to Blank Lipo-treated CSCs (Fig. 5). Also, incubation of CSCs with ILipo-SR decreased the protein level of FASN and β-catenin compared to Blank Lipo-treated CSCs. Nonetheless, protein levels of FASN and β-catenin

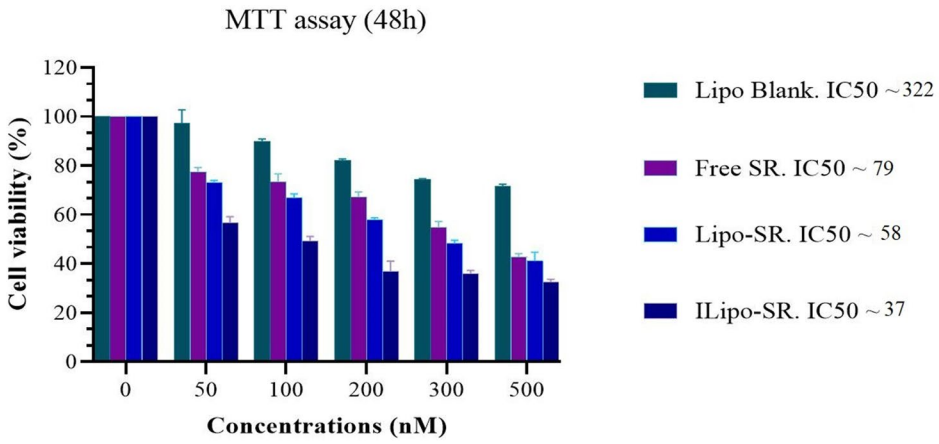

Fig. 4 In vitro CD133 + CSCs cytotoxicity of free SR and SR formulations at various concentrations (mean ± SD, $n = 3$) after 48 h using MTT assay involving absorbance. Data confirmed a dose-dependent activity of liposomal formulations on HT-29-isolated CSCs

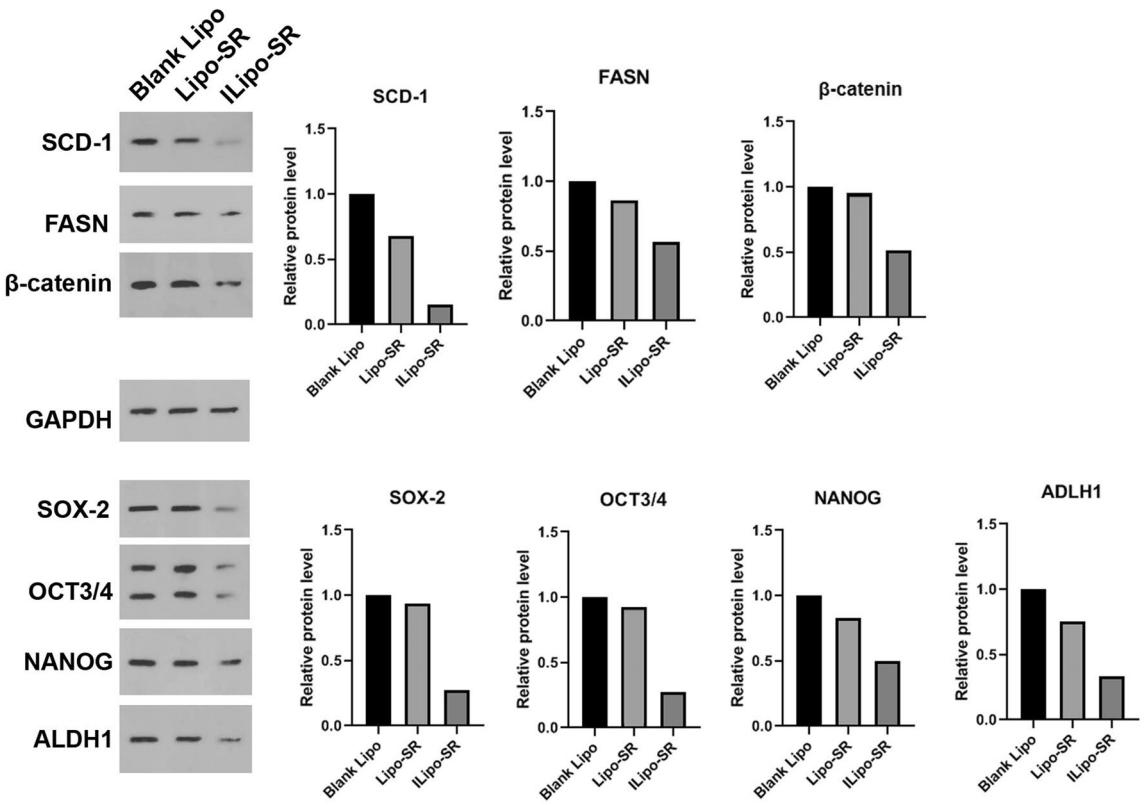

Fig. 5 Protein levels of SCD1, FASN, β-catenin, SOX-2, OCT 3/4, NANOG, and ALDH1 were determined by western blotting in CSCs after incubation with Blank Lipo, Lipo-SR, and ILipo-SR at their IC50 concentration for 48 h. LXR inhibitory SR9243(SR)-loaded liposomal formulations reduce factors associated with lipogenesis, WNT pathway, and stemness in CD133 + CSCs

were not altered after CSCs were exposed to non-targeted Lipo-SR. Calling attention, the ILipo encapsulating SR led to a much more significant reduction of the protein levels of stemness biomarkers (ALDH1, NANOG, SOX2, and OCT4) compared with Blank Lipo- and Lipo-SR- treated CSCs after 48 h (Fig. 5). These data showed that LXR inhibition especially when selected drug delivered by anti-CD133 mAb-coated ILipo could decrease the protein levels of factors associated with lipogenesis, survival, and stemness.

Lipo-SR and ILipo-SR reduced clonogenic capacity in CSCs

According to the negative effects of Lipo-SR and ILipo-SR on CSCs growth and viability (Fig. 4), and reduction

of stemness markers-supporting colony formation (Fig. 5), we investigated whether LXR inhibition using both free SR and Lipo-formulated SR could modulate the clonogenic capacity of CSCs. Based on data (Fig. 6a), the incubation of CSCs with the free SR, Lipo-SR, and ILipo-SR significantly decreased the number of colonies after 48 h compared with the control, Blank liposomes ($p < 0.001$). In addition, the encapsulation of SR by liposomes and Immunoliposomes led to a much more significant reduction of colony formation compared with free SR ($p < 0.001$). Taken together, these data showed that inhibition of LXR suppressed clonogenic capacity and malignancy of CSCs.

Liposomal SR encapsulation increased ROS content in CSCs

We investigated whether targeting LXR could alter the ROS content by using DCFH-DA-based FCM assay after treatment of CSCs with IC_{50} concentration of free SR and nano-formulations. Compared to the Blank Lipo, increased fluorescence intensity was indicated in CSCs free treated with free SR and SR-loaded Lipo/ILipo; showing the inhibition of LXR resulted in the accumulation of ROS in CSCs ($p < 0.0001$) (Fig. 6b). Compared to the free SR, CD133-targeting ILipo-SR more promoted ROS generation in CSCs after 48 h of treatment ($p < 0.05$). However, no significant differences were observed between the fluorescence intensity in free SR, and Lipo-SR treated CSCs groups ($p > 0.05$). Also, no significant differences were observed between the fluorescence intensity in Lipo-SR and ILipo-SR treated CSCs ($p > 0.05$) (Fig. 6b). These results suggest that both free and liposomal formulations of SR can induce ROS generation, and delivery of SR using ILipo conjugated with anti-CD133 antibodies exerting more ROS accumulation which could hamper the survival of $CD133^+$ CR-CSCs.

Liposomal SR formulation promoted apoptosis in CSCs

Apoptotic effects of SR-encapsulated liposomes and CD133-targeting Immunoliposomes were tested on CR-CSCs by FACS and compared with other SR formulations including free SR and blank liposomes. Empty liposomes showed a very low cytotoxic effect (or early apoptosis) (5.42%), which might duo the cytotoxic component that is used in a liposomal structure (Fig. 7). Results showed that free SR induced early apoptosis (50.2%), and late apoptosis (5.67%) of the CSCs. More than free SR, the Lipo-SR induced early apoptosis (50.2% *vs*. 55.9%), while lower than free SR, Lipo-SR induced late apoptosis (5.67% *vs*. 1.26%) of the CSCs in a concentration-dependent manner. As indicated, the percentage of early apoptosis of CSCs by ILipo-SR slightly

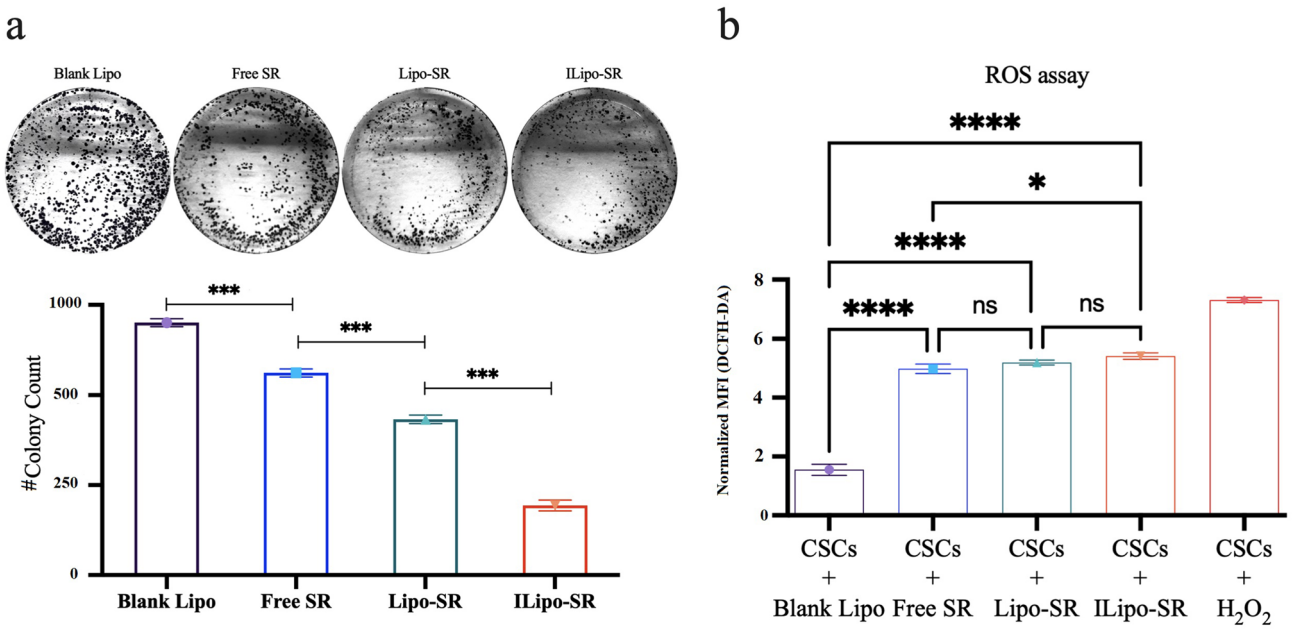

Fig. 6 **a** Free SR and SR-loaded liposomes suppressed clonogenicity in HT-29 CSCs. The number of colonies was significantly decreased ($p < 0.001$) in six-well plates after treatment with free and SR-loaded liposomes/Immunoliposomes in their IC50 value, compared to the control group (or blank Lipo). **b** FCM assay of ROS in CSCs after being treated with SR-loaded Lipo formulations. DCFH-DA assay showed significant increases in fluorescence intensity in CSCs after exposure to 79 nM free SR, 58 nM Lipo-SR and 37 nM ILipo-SR, indicating increased ROS content after the liposomal formulation of LXR inhibitor (SR, SR9243). MFI, mean fluorescence intensity; ns, non-significant. The data represent mean ± SD ($n = 3$) SD, standard deviation; *$p < 0.05$, ***$p < 0.001$, and ****$p < 0.0001$

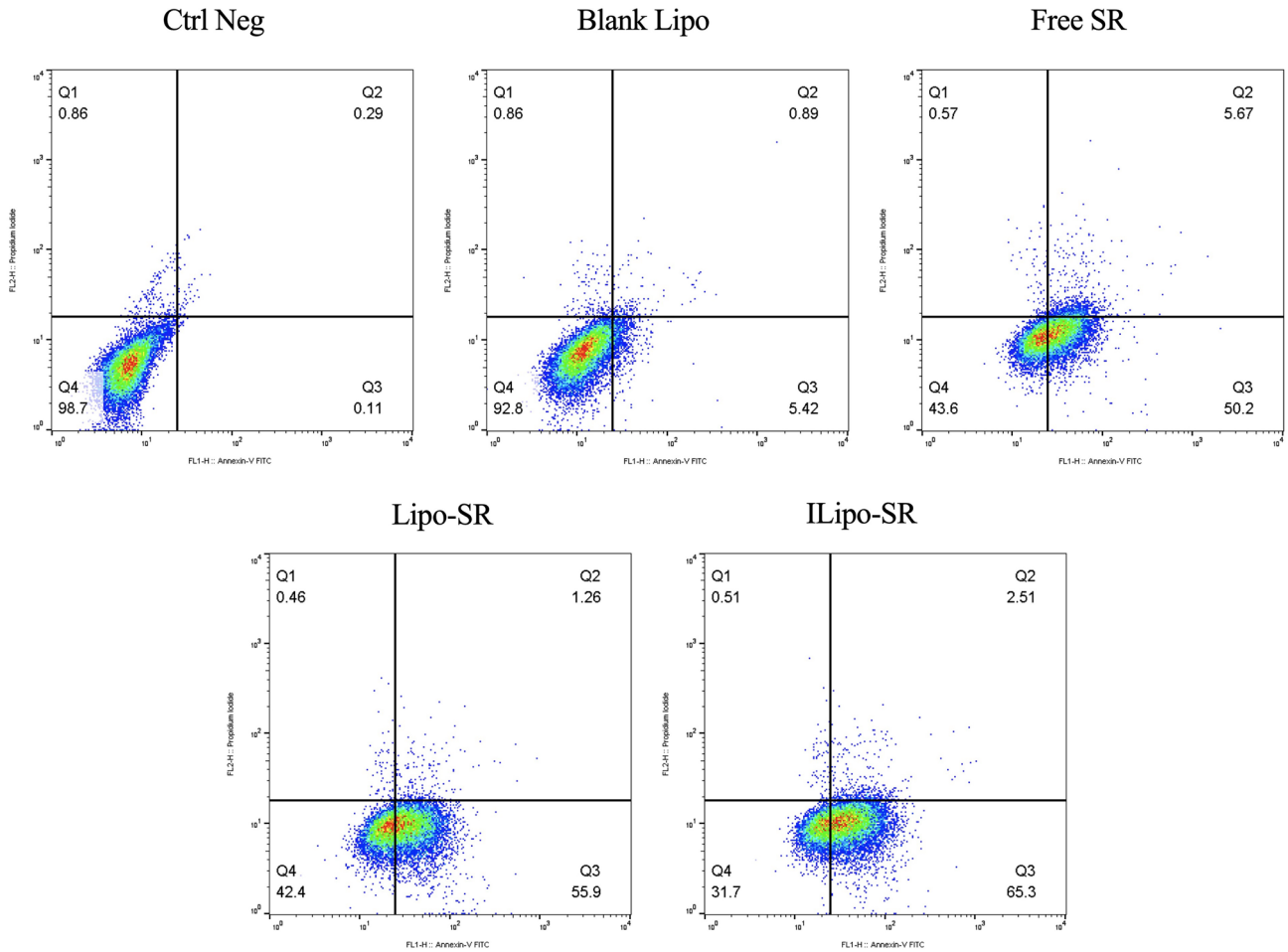

Fig. 7 FACS analysis to determine the apoptotic effect of free SR and SR in various liposomal formulations in isolated CSCs. The percentages of the early apoptosis and total cell death slightly increased through Lipo encapsulation of SR, and targeting CD133 using ILipo-SR led to a much greater enhancement in apoptosis-derived CSCs death. Live CSCs were considered as Annexin V neg/PI neg events. CSCs in early apoptosis were considered as Annexin V + /PI − . CSCs in late apoptosis were considered as Annexin V + /PI + and, finally, necrotic CSCs were considered as Annexin V − /PI +

increased compared with that by free SR (65.3% *vs*. 50.2%) and Lipo-SR (65.3% *vs*. 55.9%) (Fig. 7). These results mirrored results from the MTT assay (Fig. 4), and indicate that the free SR and Lipo-SR can induce apoptotic cell death in $CD133^{+}$CSCs. This effect is intensified by using Immunoliposomes.

Discussion

CSCs exhibit tumor-promoting properties such as drug resistance, dormancy, recurrence, and metastasis [10, 21, 22]. Cancer therapy using chemo agents encountered non-specific delivery/action, uncontrollable drug concentration at the tumor site, and poor solubility [23]. Target-directed liposomes are the most promising to overcome the drug limitation [24], and CD133 is a CSC-surface biomarker that can maintain CSCs in an undifferentiated state [8]. Therefore, MACS technology enriched $CD133^{+}$CSC-like phenotype in high purity as the target cells to increase the efficacy of liposomal drug delivery. Moreover, LXR activation can upregulate the transcription of target genes participating in lipogenesis and stemness, [5, 25–27], and thus, using LXR reverse agonist SR9243 (SR)-loaded PEGylated Immunoliposomes (ILipo-SR) should be a suitable candidate to suppress CSCs tumorigenesis. Indeed, tumor cells display high metabolic activity (i.e., glycolysis and lipogenesis) with high LXR activity and SR9243 has the potential to downregulate the LXR expression and reduce SREBP-1c-, FASN- and SCD-driving metabolic activities in tumor cells. LXR inverse agonist SR9243 induces interactions between LXR and co-repressors and thus, inhibits the transcription of target genes by LXR [17].

In the present study, the designed Lipo or ILipo showed full encapsulation of SR, indicating that the encapsulation efficiency increased at nanomolar concentrations of SR, and functionalization of liposomes with anti-CD133 mAb did not interfere with SR loading. DLS analysis showed the Lipo-SR/ILipo-SR average diameter of approximately 63.79 nm, which was revealed to be suitable and practical for drug delivery. The surface morphologies of Lipo-SR and ILipo-SR investigated by TEM revealed a uniform spherical shape. Both of Lipo-SR and ILipo-SR showed positive zeta potential, but compared to Lipo-SR, the zeta potential of ILipo-SR is lower, confirming that the anti-CD133 mAbs conjugation have slightly modified the surface charge of ILipo-SR. The non-significant differences between the size and zeta of Lipo-SR and ILipo-SR are consistent with a study that has shown the incorporation of the peptide antigen did not influence the size and zeta potential results of CLs [28]. Notably, CLs are water solubility and their flexibility and high cationic charge density provide their interaction with negatively charged cancer cell surfaces and improve their cellular binding as well uptake into target cells [29]. Nonetheless, CLs can induce protein corona resulting in their rapid clearance in vivo [30], that conjugated anti-CD133 mAbs and the stealth effect produced by mPEG-2000 can reduce exposed charges to extend storage stabilities or improve the circulation time in the body. In addition, DOPE-containing CLs presented a neutral charge at physiological pH, which improved their circulation and reduced their toxicity [30].

Besides ionic interaction, the specific overexpression of cell surface antigen selected ligand plays a critical role in immunoliposomal therapy [10, 31]. The binding ability of CD133-ILipo is positively related to the CD133 expression level on HT-29 cells in vitro, and we indicated that the binding of anti-CD133 mAb-FITC to CD133 antigen lead to enhancement of the cellular binding, and subsequently led to significantly increased endocytosis and uptake of ILipo-RhoB in $CD133^+$CSCs. Moreover, the interaction between the cationic DOTAP and endosomal/lysosomal membranes-anionic molecules increased their permeability and thus can contribute to the release of drugs at low pH [32].

More efficient than Lipo-SR and free SR, the ILipo-SR induced cellular toxicity and inhibited the CSCs proliferation at lower concentrations with acceptable safety profiles. Compared to differentiated cancer cells, glioblastoma CSCs (GSCs) [33] and $CD133^+$CR-CSCs [34] exhibited higher lipogenesis, and we showed the dual targeting of the CD133 and LXR pathway using ILipo-SR reduced the expression of lipogenesis FASN and SCD-1 enzymes in $CD133^+$CR-CSCs. Inhibition of lipogenesis resulted in reducing the expression of stemness-driving factors including β-catenin, ALDH1, NANOG, SOX2, and OCT4, which is resealable results as FASN and SCD-1 play pivotal roles in the maintenance of stemness in $CD133^+$GSCs, ovarian $ALDH^+/CD133^+$CSCs, and lung $ALDH1A1^+$TICs (tumor-initiating cells) [3, 33, 35].

Stemness, active de novo lipogenesis, and high levels of lipid droplets are distinctive marks of $CD133^+$GSCs and $CD133^+$CR-CSCs [33, 36], thus, inhibition of those properties upon LXR suppression using both free and liposomal SR formulations lead to a decrease in CSC clonogenicity and self-renewal capacity. Moreover, cholesterol synthesis as an active metabolic pathway promotes the sphere-forming cells [37], and therefore, targeting LXR signaling as a regulator of cholesterol biosynthesis could be decreased colony formation in CSCs, as we indicated. Fatty acid metabolism maintained ROS at a minimum level in human stem cells [38], and targeting LXR as a regulator of lipogenesis is expected to enhance ROS generation in $CD133^+$CSCs as an FCM assay confirmed this result. Moreover, *Nanog*-silenced TICs promoted the accumulation of ROS and reduced spheroid formation [39, 40], consistent with this study that reduction of CSC stemness factor enhanced ROS production and reduced colony formation.

Finally, the FCM assay indicated that targeting the LXR pathway induced early apoptosis in CSCs. This event enhanced upon encapsulation of SR in Lipo and ILipo, while late apoptosis was reduced. The low ROS niche and active lipogenesis support the stemness and self-renewal capacity of CSCs [6, 33], and induced apoptosis could be explained by produced ROS and inhabited cell metabolism and stemness. SR9243 downregulated the fatty acid synthesis as well as intracellular fatty acid content and thus, caused membrane structural function disruption and apoptosis induction in cancerous cells [41]. SR9243 also induced the PPP1R15A expression, which promoted apoptosis by inducing the phosphorylation of TP53 [42]. Moreover, the SCD-1 downregulation leads to induction of palmitic acid-induced toxicity and unfolded protein response in the endoplasmic reticulum, and also an increase in membrane-saturated fatty acids-inducing apoptosis [43]. In summary, according to our cellular association studies, more efficient than free SR and Lipo-SR, the internalized ILipo-SR has shown potentially exerted their anticarcinogenic properties through modulation LXRs activity as well downstream events. There are some limitations in this study that demand more evaluation of ILipo-SR anticancer effects on the CSC-xenographted model, as in vitro experiments cannot be fully used to predict the behavioral changes of nanoparticles in vivo.

Conclusion

Herein, we developed an ILipo-SR delivery system. Results conformed dual targeting of CD133 as a stem biomarker, and the LXR signaling pathway as a regulator of lipogenesis

could alter the activity of CR-CSCs. According to the FCM assay, more effective than non-targeted liposomes, receptor-ligand interaction improved the cell binding and uptake of ILipo. The biological cell culture studies demonstrated cationic ILipo encapsulating SR significantly reduced CSCs tumorigenesis and induced apoptosis in $CD133^{+}$CSCs in vitro. In conclusion, these results suggest that anti-CD133 mAb-conjugated PEGylated ILipo-SR can be considered a potential platform to target CD133 antigen and metabolic program of CSCs, and could be investigated in further in vivo drug delivery evaluations.

Acknowledgements The authors appreciate the personnel of Drug Applied Research Center for help and guide.

Author contributions HDM, and SAR performed experiments and prepared draft. MN, RR, and HH designed and supervised the study. All the authors read and approved the final manuscript.

Funding This work was financially supported by Tabriz University of Medical Sciences (Hassan Dianat-Moghadam Ph.D. Thesis. Approval ID: IR.TBZMED.VCR.REC.1397.097).

Data availability The data that support the findings of this study are available from the corresponding authors upon reasonable request.

Declarations

Competing interests The authors declare that there is no conflict of interest.

Ethical approval Not applicable.

Consent for publication All authors agree with the publication of this manuscript in this journal.

References

1. Ehmsen S, Pedersen MH, Wang G, Terp MG, Arslanagic A, Hood BL, et al. Increased cholesterol biosynthesis is a key characteristic of breast cancer stem cells influencing patient outcome. Cell Rep. 2019;27(13):3927-38.e6.
2. Li H, Feng Z, He M-L. Lipid metabolism alteration contributes to and maintains the properties of cancer stem cells. Theranostics. 2020;10(16):7053.
3. Li J, Condello S, Thomes-Pepin J, Ma X, Xia Y, Hurley TD, et al. Lipid desaturation is a metabolic marker and therapeutic target of ovarian cancer stem cells. Cell Stem Cell. 2017;20(3):303-14.e5.
4. Fu T, Coulter S, Yoshihara E, Oh TG, Fang S, Cayabyab F, et al. FXR regulates intestinal cancer stem cell proliferation. Cell. 2019;176(5):1098–112.
5. Dianat-Moghadam H, Khalili M, Keshavarz M, Azizi M, Hamishehkar H, Rahbarghazi R, et al. Modulation of LXR signaling altered the dynamic activity of human colon adenocarcinoma cancer stem cells in vitro. Cancer Cell Int. 2021;21(1):100.
6. Jagust P, de Luxán-Delgado B, Parejo-Alonso B, Sancho P. Metabolism-based therapeutic strategies targeting cancer stem cells. Front Pharmacol. 2019;10:203.
7. Ferrand A, Sandrin MS, Shulkes A, Baldwin GS. Expression of gastrin precursors by CD133-positive colorectal cancer cells is crucial for tumour growth. Biochimica et Biophys Acta (BBA)—Mol Cell Res. 2009;1793(3):477–88.
8. Wang BB, Li ZJ, Zhang FF, Hou HT, Yu JK, Li F. Clinical significance of stem cell marker CD133 expression in colorectal cancer. Histol Histopathol. 2016;31(3):299–306.
9. Rappa G, Fargeas CA, Le TT, Corbeil D, Lorico A. Letter to the editor: an intriguing relationship between lipid droplets, cholesterol-binding protein CD133 and Wnt/β-catenin signaling pathway in carcinogenesis. Stem Cells. 2015;33(4):1366–70.
10. Dianat-Moghadam H, Heidarifard M, Jahanban-Esfahlan R, Panahi Y, Hamishehkar H, Pouremamali F, et al. Cancer stem cells-emanated therapy resistance: implications for liposomal drug delivery systems. J Control Release. 2018;288:62–83.
11. Shen Y-A, Li W-H, Chen P-H, He C-L, Chang Y-H, Chuang C-M. Intraperitoneal delivery of a novel liposome-encapsulated paclitaxel redirects metabolic reprogramming and effectively inhibits cancer stem cells in Taxol®-resistant ovarian cancer. Am J Trans Res. 2015;7(5):841.
12. Biju V. Chemical modifications and bioconjugate reactions of nanomaterials for sensing, imaging, drug delivery and therapy. Chem Soc Rev. 2014;43(3):744–64.
13. Arabi L, Badiee A, Mosaffa F, Jaafari MR. Targeting CD44 expressing cancer cells with anti-CD44 monoclonal antibody improves cellular uptake and antitumor efficacy of liposomal doxorubicin. J Control Release. 2015;220:275–86.
14. Alshaer W, Hillaireau H, Vergnaud J, Ismail S, Fattal E. Functionalizing liposomes with anti-CD44 aptamer for selective targeting of cancer cells. Bioconjug Chem. 2014;26(7):1307–13.
15. Ning S-T, Lee S-Y, Wei M-F, Peng C-L, Lin SY-F, Tsai M-H, et al. Targeting colorectal cancer stem-like cells with anti-CD133 antibody-conjugated SN-38 nanoparticles. ACS Appl Mater Interfaces. 2016;8(28):17793–804.
16. Ganesh S, Iyer AK, Morrissey DV, Amiji MM. Hyaluronic acid based self-assembling nanosystems for CD44 target mediated siRNA delivery to solid tumors. Biomaterials. 2013;34(13):3489–502.
17. Carpenter KJ, Valfort A-C, Steinauer N, Chatterjee A, Abuirqeba S, Majidi S, et al. LXR-inverse agonism stimulates immune-mediated tumor destruction by enhancing CD8 T-cell activity in triple negative breast cancer. Sci Rep. 2019;9(1):1–18.
18. Chen Z, Moon JJ, Cheng W. Quantitation and stability of protein conjugation on liposomes for controlled density of surface epitopes. Bioconjug Chem. 2018;29(4):1251–60.
19. Yang D, Correia JJ, Stafford WF III, Roberts CJ, Singh S, Hayes D, et al. Weak IgG self-and hetero-association characterized by fluorescence analytical ultracentrifugation. Protein Sci. 2018;27(7):1334–48.
20. Schneider M, Huber J, Hadaschik B, Siegers GM, Fiebig H-H, Schüler J. Characterization of colon cancer cells: a functional approach characterizing CD133 as a potential stem cell marker. BMC Cancer. 2012;12(1):96.
21. Dianat-Moghadam H, Sharifi M, Salehi R, Keshavarz M, Shahgolzari M, Amoozgar Z. Engaging stemness improves cancer immunotherapy. Cancer Lett. 2022;554:216007.
22. Dianat-Moghadam H, Mahari A, Salahlou R, Khalili M, Azizi M, Sadeghzadeh H. Immune evader cancer stem cells direct the perspective approaches to cancer immunotherapy. Stem Cell Res Ther. 2022;13(1):1–12.
23. Dianat-Moghadam H, Heidarifard M, Mahari A, Shahgolzari M, Keshavarz M, Nouri M, et al. TRAIL in oncology: From recombinant TRAIL to nano- and self-targeted TRAIL-based therapies. Pharmacol Res. 2020;155:104716.
24. Obeid MA, Tate RJ, Mullen AB, Ferro VA. Lipid-based nanoparticles for cancer treatment Lipid Nanocarriers for Drug Targeting. Netherlands: Elsevier; 2018. p. 313–59.

25. Flaveny CA, Griffett K, El-Gendy BE-DM, Kazantzis M, Sengupta M, Amelio AL, et al. Broad anti-tumor activity of a small molecule that selectively targets the Warburg effect and lipogenesis. Cancer Cell. 2015;28(1):42–56.
26. Uno S, Endo K, Jeong Y, Kawana K, Miyachi H, Hashimoto Y, et al. Suppression of β-catenin signaling by liver X receptor ligands. Biochem Pharmacol. 2009;77(2):186–95.
27. Agarwal JR, Wang Q, Tanno T, Rasheed Z, Merchant A, Ghosh N, et al. Activation of liver X receptors inhibits hedgehog signaling, clonogenic growth, and self-renewal in multiple myeloma. Mol Cancer Ther. 2014;13(7):1873–81.
28. Soema PC, Willems G-J, Jiskoot W, Amorij J-P, Kersten GF. Predicting the influence of liposomal lipid composition on liposome size, zeta potential and liposome-induced dendritic cell maturation using a design of experiments approach. Eur J Pharm Biopharm. 2015;94:427–35.
29. Laouini A, Jaafar-Maalej C, Limayem-Blouza I, Sfar S, Charcosset C, Fessi H. Preparation, characterization and applications of liposomes: state of the art. J Colloid Sci Biotechnol. 2012;1(2):147–68.
30. Majzoub RN, Chan C-L, Ewert KK, Silva BFB, Liang KS, Jacovetty EL, et al. Uptake and transfection efficiency of PEGylated cationic liposome–DNA complexes with and without RGD-tagging. Biomaterials. 2014;35(18):4996–5005.
31. Mahmoudi R, Dianat-Moghadam H, Poorebrahim M, Siapoush S, Poortahmasebi V, Salahlou R, et al. Recombinant immunotoxins development for HER2-based targeted cancer therapies. Cancer Cell Int. 2021;21:1–17.
32. Wattiaux R, Jadot M, Warnier-Pirotte M-T, Wattiaux-De CS. Cationic lipids destabilize lysosomal membrane in vitro. FEBS Lett. 1997;417(2):199–202.
33. Yasumoto Y, Miyazaki H, Vaidyan LK, Kagawa Y, Ebrahimi M, Yamamoto Y, et al. Inhibition of fatty acid synthase decreases expression of stemness markers in glioma stem cells. PLoS ONE. 2016;11(1):e0147717.
34. Semenza GL. Hypoxia-inducible factors: coupling glucose metabolism and redox regulation with induction of the breast cancer stem cell phenotype. EMBO J. 2017;36(3):252–9.
35. Noto A, Raffa S, De Vitis C, Roscilli G, Malpicci D, Coluccia P, et al. Stearoyl-CoA desaturase-1 is a key factor for lung cancer-initiating cells. Cell Death Dis. 2013;4(12):e947-e.
36. Tirinato L, Liberale C, Di Franco S, Candeloro P, Benfante A, La Rocca R, et al. Lipid droplets: a new player in colorectal cancer stem cells unveiled by spectroscopic imaging. Stem cells. 2015;33(1):35–44.
37. Liu M, Xia Y, Ding J, Ye B, Zhao E, Choi J-H, et al. Transcriptional profiling reveals a common metabolic program in high-risk human neuroblastoma and mouse neuroblastoma sphere-forming cells. Cell Rep. 2016;17(2):609–23.
38. Ito K, Suda T. Metabolic requirements for the maintenance of self-renewing stem cells. Nat Rev Mol Cell Biol. 2014;15(4):243–56.
39. Chen C-L, Uthaya Kumar Dinesh B, Punj V, Xu J, Sher L, Tahara Stanley M, et al. NANOG metabolically reprograms tumor-initiating stem-like cells through tumorigenic changes in oxidative phosphorylation and fatty acid metabolism. Cell Metab. 2016;23(1):206–19.
40. Dianat-Moghadam H, Mahari A, Heidarifard M, Parnianfard N, Pourmousavi-Kh L, Rahbarghazi R, et al. NK cells-directed therapies target circulating tumor cells and metastasis. Cancer Lett. 2021;497:41–53.
41. Wu G, Wang Q, Xu Y, Li J, Zhang H, Qi G, et al. Targeting the transcription factor receptor LXR to treat clear cell renal cell carcinoma: agonist or inverse agonist? Cell Death Dis. 2019;10(6):416.
42. Connor JH, Weiser DC, Li S, Hallenbeck JM, Shenolikar S. Growth arrest and DNA damage-inducible protein GADD34 assembles a novel signaling complex containing protein phosphatase 1 and inhibitor 1. Mol Cell Biol. 2001;21(20):6841–50.
43. Ariyama H, Kono N, Matsuda S, Inoue T, Arai H. Decrease in membrane phospholipid unsaturation induces unfolded protein response*. J Biol Chem. 2010;285(29):22027–35.